Adsorption of boron on Si(111): Physics, chemistry, and atomic-scale electronic devices

Ph. Avouris, In-Whan Lyo, F. Bozso, and E. Kaxiras
IBM Research Division, T. J. Watson Research Center, Yorktown Heights, New York 10598

(Received 27 November 1989; accepted 8 January 1990)

We have used scanning tunneling microscopy, atom-resolved tunneling spectroscopy, and photoemission to investigate the interaction of B with Si(111). Using decaborane as the source of B, we have followed the structural and electronic modifications of the surface as a function of the annealing temperature. In the stable B/Si(111)-$\sqrt{3}\times\sqrt{3}$ surface, B occupies a novel configuration where it substitutes for a Si atom in the 3rd atomic layer directly below a Si adatom. Because of a Si-to-B charge transfer, the top Si adatom layer has no occupied dangling-bond states and is insulating. As a result, the chemical properties of Si adatoms on the B/Si(111)-$\sqrt{3}\times\sqrt{3}$ surface are very different from those of the adatoms on the Si(111)-7×7 surface. We find evidence for doping effects on chemistry that involve short-range direct dopant-reactive site interactions. Finally, we report on the electrical characteristics of localized defect sites on the B-doped Si surface. We found that I–V curves over such sites may show regions of negative differential resistance and that this behavior is localized in areas of atomic dimensions (~ 1 nm). We propose a model according to which the development of negative resistance requires the existance of narrow peaks at appropriate energies in the density of states spectra of both sample and tip.

I. INTRODUCTION

Scanning tunneling microscopy (STM)[1] has been proven to be a powerful technique for the real-space imaging of surfaces and adsorbed layers with atomic resolution.[2] In addition, the local valence electronic structure can be studied using atom-resolved tunneling spectroscopy (ARTS).[3] The combination of STM and ARTS allows the study, on the atomic scale, of more complex surface phenomena such as surface chemistry and the determination of the electrical properties of local chemical structures.

In this article we demonstrate these new capabilities in a study of the adsorption of boron on Si(111). Specifically, we use STM, ARTS, and photoemission to address the following questions: (a) Where do the B atoms reside and what makes them choose that particular configuration? (b) How does the presence of B dopant atoms affect the electronic structure and chemistry of the Si surface? (c) What are the electrical characteristics of local surface structures, and how small can electronic devices be made using such structures?

II. THE ADSORPTION SITE OF BORON ON Si(111)

There has been a lot of interest in understanding the factors that determine chemisorption sites on Si surfaces. The chemisorption of group III atoms such as Al,[4] Ga,[5] and In[6] on Si(111) has been studied by STM and other techniques. In all cases it was found that the goup III atom occupies an adatom position at a T_4 site of the Si(111) surface. The identification of the adsorption site of boron on Si(111) is particularly important because of its common use as a dopant of Si. Should B occupy an adatom T_4 site? Al, Ga, and In are all larger that Si, while B is significantly smaller (Si covalent radius: 1.11 Å, B: 0.82 Å). As a result of boron's small size, the short B–Si bonds will induce considerable tensile strain and will bring the B atom very close to the second layer Si atom below the T_4 site, leading to strong overlap repulsion.

To decipher the preferred site of B adsorption we have performed STM, ARTS, ultraviolet photoemission (UPS), x-ray photoemission (XPS), and ion-scattering (ISS) spectroscopic measurements. An analysis leading to the identification of the adsorption site has been presented elsewhere,[7] so here we will review only the essential points. As a source of B in our studies we have used a molecular precursor, decaborane-14 ($B_{10}H_{14}$, DB). The STM and ARTS experimental set-ups and Si sample preparation techniques have been described in detail elsewhere.[8]

In Fig. 1 we show a topograph of the Si(111)-7×7 surface after exposure at 300 K to 0.2 L (1 L = 10^{-6} Torr s) of DB.

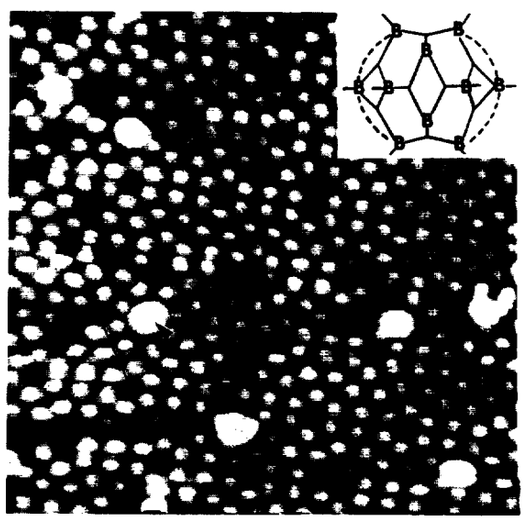

FIG. 1. STM topograph of a Si(111)-7×7 surface exposed to 0.2 L of decaborane (sample bias = +2V). A 7×7 unit cell containing an adsorbed molecule is outlined. The inset shows a projection of the decaborane molecule along the C_5 axis.

 0734-2101/90/043405-07$01.00

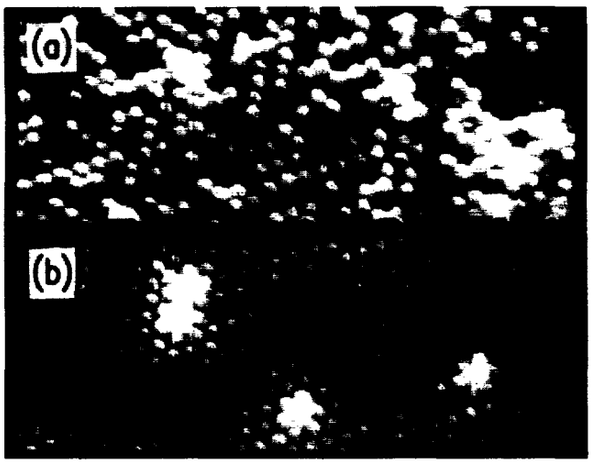

FIG. 2. STM topographs of the surfaces produced by exposing Si(111)-7×7 to (a) 0.4 L of decaborane at 300 K and briefly annealing to 800 °C, and (b) 1 L of decaborane and annealing to 1000 °C. Sample bias = +2V.

In the inset, a projection along the C_2 axis of the structure of the DB molecule is shown. It is clear that STM can image these molecules which appear as round disks in Fig. 1. The DB molecules adsorb preferentially on defects and on center-adatoms of the 7×7 surface. Upon annealing to temperatures above 800 K the hydrogen desorbs and we are left with only boron on the silicon surface. In Fig. 2(a) we show a topograph of the unoccupied states of a surface produced by exposing the 7×7 surface at 300 K to 0.4 L of DB and briefly annealing to ~1000 K. Overall, the surface has a $\sqrt{3}\times\sqrt{3}$

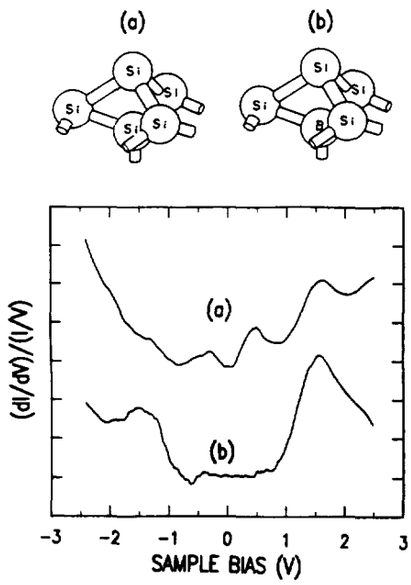

FIG. 3. Top: Local structures of (a) a Si adatom on a T_4 site; (b) the proposed equilibrium structure involving B in a substitutional site under a Si-T_4 adatom. Bottom: Atom-resolved tunneling spectra obtained over (a) a Si-T_4 adatom site (bright site) of Figs. 2(a), and 2(b) over a majority site of Fig. 2(b). Sample bias = +2V.

structure. However, some of the atomic sites appear bright (high) while others are dark (low). ARTS studies show that the spectra over bright sites [Fig. 3(a)] are essentially identical to those of Si-T_4 adatoms [see local structure in Fig. 3(a) top] on the 7×7 surface.[8] Studies of the topography as a function of bias suggest that the majority of the darker sites correspond to B-T_4 adatoms. The B-T_4 adatoms appear darker because, according to our calculations,[7] the B adatoms are 0.4 Å lower than the Si adatoms and their wave function is more contracted.

Although it appears that B behaves very much like the other group III elements, i.e., it occupies a T_4 adatom site, our local density functional (LDF) slab-calculations[7] suggest that this configuration is not the most stable one. We have performed total energy calculations on a variety of structures. We found that the lowest energy structure is that shown at the top of Fig. 3(b). This structure involves B in a substitutional site at the second Si layer and a Si adatom in a T_4 site directly over it. This structure was found to be about 1 eV per $\sqrt{3}\times\sqrt{3}$ unit cell more stable than the B-T_4 configuration. Its stability is due to the fact that the substitutional B atom does not induce subsurface strain and each Si adatom eliminates three surface dangling bands (dbs) while introducing a new one. Because of the proximity of the B atom and the Si adatom (~2.2 Å) and the higher electronegativity of B, the db state of the Si adatom is emptied by charge transfer to B, thus further reducing the energy of this configuration. Although the substitutional site is most stable, its formation involves the breaking of bonds and for this reason the B-T_4 site is kinetically favored. If the sample is properly annealed, however, the substitutional configuration [Fig. 3(b) top] should be formed. Indeed, by annealing a sample exposed to 1 L of DB to ~1300 K we obtain a uniform surface [Fig. 2(b)] whose top layer, according to our ISS measurements, is composed of Si atoms. The B is still very near the surface, however, as shown by the fact that the B(1*s*) XPS intensity is little changed upon annealing. The ARTS spectrum, Fig. 3(b), shows that this surface is insulating with a prominent unoccupied band at about 1.5 eV above E_F and an occupied band at about 1.5 eV below E_F. According to the calculations these states have dangling-bond and back-bond character, respectively. Thus, all available evidence suggests that the equilibrium configuration shown in Fig. 3(b)(top) has been attained. This conclusion is further reenforced by independent studies[9,10] of B surface segregation from heavily B-doped bulk Si. In these studies the same substitutional configuration of B was identified as the most stable structure. Although intermediate, metastable configurations may be different depending on the way B is introduced (by adsorption from the gas-phase or diffusion from the bulk), the equilibrium configuration should be the same in both types of experiments.

III. THE EFFECT OF B ON SURFACE CHEMISTRY

The chemistry of Si surfaces depends very strongly on the local structure and strain considerations at the reactive site.[11] For example, our previous work has shown[8] that the reactivity of db sites on the Si(111)-(7×7) surface depends

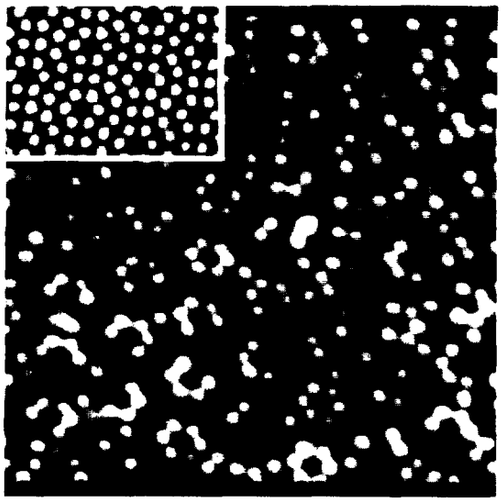

FIG. 4. STM topograph of a Si(111)-7×7 surface exposed to about 5 L of NH_3 at 300 K (sample bias + 2V). Inset: Topograph of a clean Si(111)-7×7 surface. A 7×7 unit cell is outlined in both cases.

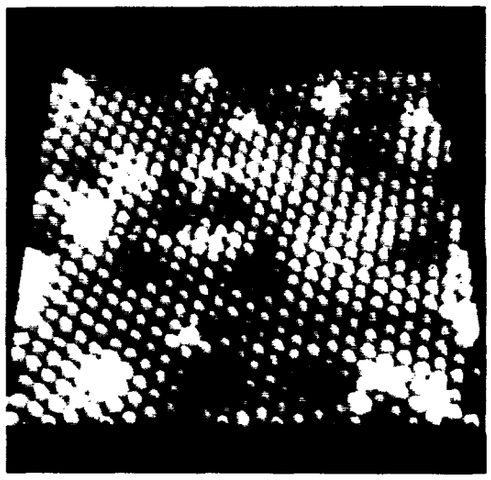

FIG. 5. STM topograph of a B/Si(111)-$\sqrt{3}\times\sqrt{3}$ surface exposed to ~400 L of NH_3 at 300 K (sample bias = + 2V).

sensitively on the occupation of the particular db level and on local lattice strain effects. As discussed above, the equilibrium configuration of the B/Si(111)-$\sqrt{3}\times\sqrt{3}$ surface involves a Si adatom top layer, with the B dopants below the Si adatoms in substitutional sites. Because of the Si-to-B charge transfer, the Si top layer of the B/Si(111)-$\sqrt{3}\times\sqrt{3}$ system has no occupied db levels. This drastic change in the db level occupancy should be reflected in the chemical properties of the surface. Indeed, we find that the top Si layer of this B/Si(111)-$\sqrt{3}\times\sqrt{3}$ surface has very different chemical properties than those of clean Si surfaces. We illustrate this using the reaction with NH_3 as an example. In Fig. 4 we show a topograph of the unoccupied states of the Si(111)-(7×7) surface (sample bias = + 1.5 V) after exposure to a few L of NH_3. In the inset, a portion of a clean 7×7 surface is shown and a 7×7 unit cell is outlined. The 12 atomic sites imaged within the unit cell correspond to the 12 Si adatom sites of the Takayanagi *et al.*[12] model of the 7×7 reconstruction. Exposure to NH_3 has led to extensive reaction among the Si adatoms. Reacted adatoms lack dbs and thus appear dark at this bias. One also observes that the surface reaction is anisotropic with most unreacted (bright) adatoms being corner adatoms, i.e., adatoms surrounding the holes or vacancies at the corners of the unit cell. This selective reaction gives rise to the ring-like structures seen in Fig. 4. The reaction on the 7×7 surface has been shown by vibrational spectroscopy[13] and photoemission[14,15] to involve the dissociation of NH_3 to NH_2 + H and the attachment of these groups to surface Si atoms.

In contrast to the above behavior, exposure of the B/Si(111)-$\sqrt{3}\times\sqrt{3}$ surface to even hundreds of L of NH_3 at room temperature leads to very little reaction. This is demonstrated in Fig. 5, which shows a topograph (bias = + 2 V) of the $\sqrt{3}\times\sqrt{3}$ surface after exposure to about 400 L of NH_3; very few reacted (dark) sites are observed. It is clear that boron incorporation had a drastic influence on the reactivity of Si adatoms. However, this influence is not simply a change in reaction rate. We find that if we cool the $\sqrt{3}\times\sqrt{3}$ surface to 90 K, the sticking of NH_3 to the surface is strongly increased. Currently, we cannot perform STM experiments at low temperatures, so we have studied the interaction of $\sqrt{3}\times\sqrt{3}$ surface with NH_3 using UPS. Figure 6 shows that exposure of the Si(111)-(7×7) surface at 90 K to 2 L of NH_3 gives a spectrum which is dominated by two strong bands from physisorbed NH_3 at about 5.8 eV and 11.2 eV. These bands are due to photoemission from the NH_3 lone-pair orbital and N–H bonding orbitals, respectively.[14,15] Upon annealing to 350 K we obtain a spectrum showing two new red-shifted bands. The band at ~4.5 eV has been as-

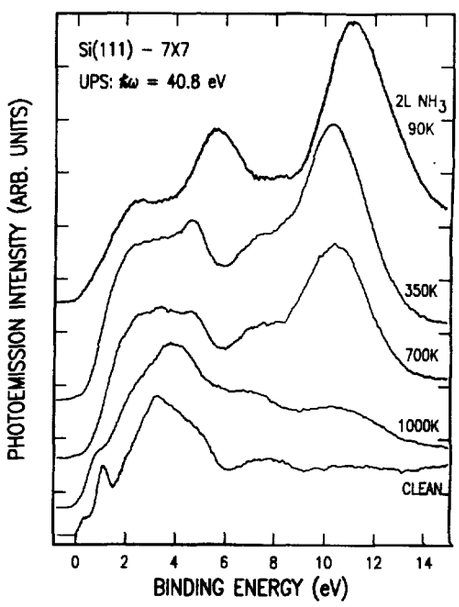

FIG. 6. He II valence photoemission spectra of the surfaces produced by the interaction of clean Si(111)-7×7 with 2 L of NH_3 at 90 K followed by annealing to the indicated temperatures.

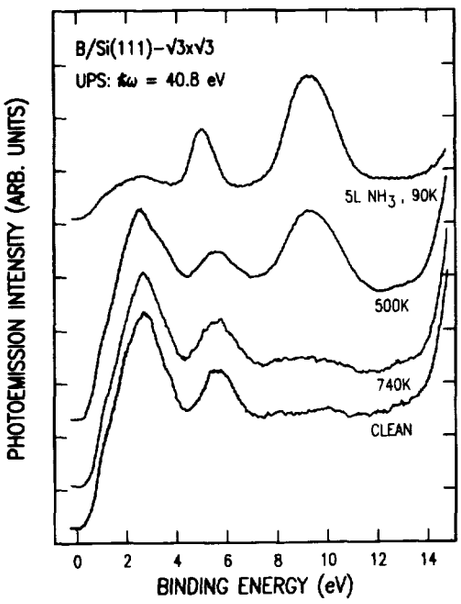

FIG. 7. He II valence photoemission spectra of the surfaces produced by the interaction of a B/Si(111)-$\sqrt{3}\times\sqrt{3}$ surface with 5 L of NH_3 at 90 K and subsequently annealing to the indicated temperatures.

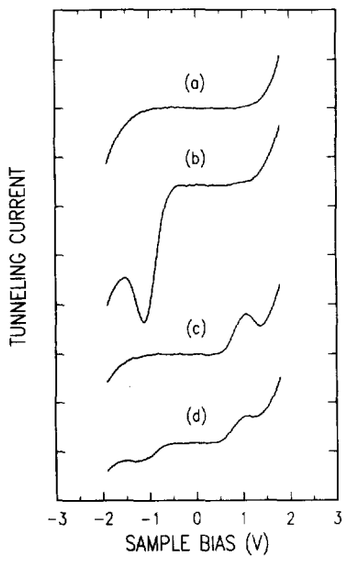

FIG. 8. Tunneling current versus sample bias (I–V) curves. (a) Normal I–V curve obtained over a majority site of the B/Si(111)-$\sqrt{3}\times\sqrt{3}$ surface. Curves (b) to (d) have been obtained over defect sites and illustrate the different types of negative differential resistance behavior observed in our studies.

signed by Kubler *et al.*[13] to the Si–NH_2 species formed upon dissociation of NH_3, while the $\sim$10.3 eV band is due to emission from N–H levels. These features are still present at 700 K, while heating to 1000 K leads to hydrogen desorption and the formation of silicon nitride, which is characterized by broad bands at about 4, 7, and 10.5 eV.[15] In Fig. 7 we show the corresponding behavior of the B/Si(111)-$\sqrt{3}\times\sqrt{3}$ surface. Exposure to NH_3 at 90 K gives rise to a UPS spectrum characteristic of the NH_3 molecule. Annealing to 500 K, however, does not give rise to the red-shifted bands characteristic of Si–NH_2 species. Moreover, the adsorption process is reversible. Heating to 740 K leads to the desorption of molecular NH_3 and the recovery of a clean $\sqrt{3}\times\sqrt{3}$ surface. Although a firm assignment will require vibrational spectra, the above UPS results strongly suggest that the nature of the interaction of NH_3 with the 7×7 and $\sqrt{3}\times\sqrt{3}$ surfaces is very different: NH_3 dissociates at the adatom sites of the 7×7 surface while it binds molecularly to the adatom sites of the $\sqrt{3}\times\sqrt{3}$ surface by donating N lone-pair electrons to the empty db levels of the adatoms (a Lewis acid-base reaction). This is a novel doping effect on chemical reactivity where not only the reaction rate is affected by doping but the products of the reaction are also determined by it. There are several examples of doping effects on reaction rates on Si surfaces, particularly in plasma–surface reactions. Long-range mechanisms involving electric fields and band bending have been discussed.[16] More recently, chemical effects of doping have been proposed.[17,18] Our results provide a clear example of a direct short-range interaction of the dopant atom, B, with the reaction site, i.e., the adatom db. Long-range effects may also be important, and may be responsible for the observed stabilization of Si-based $\sqrt{3}\times\sqrt{3}$-islands by B doping. In this case, a shift of the Fermi level position towards the valence band leads to a decreased population of the Si-adatom dbs and thus lowers the energy of the Si(111)-$\sqrt{3}\times\sqrt{3}$ reconstruction.

IV. ATOMIC SCALE TUNNEL-DIODES INVOLVING LOCAL STRUCTURES ON THE B/Si(111) SURFACE

We next will consider the electrical characteristics of naturally occuring defect sites on the B/Si(111)-$\sqrt{3}\times\sqrt{3}$ surface. Depending on the preparation conditions (amount of DB, temperature and rate of thermal annealing) the $\sqrt{3}\times\sqrt{3}$ surface can have a variety of different point and extended defects such as those seen in Fig. 2(b). Intrigued by possible analogies with larger scale microfabricated structures such as quantum-wells and dots which are based on size quantization,[19] we explored the tunneling I–V's of such surface sites. The most interesting finding was the observation of negative differential resistance (NDR) over sites of atomic dimensions.[20] Figure 8 shows all the types of NDR behavior we observed over different defect sites during our studies. It can be seen that NDR can develop for negative, positive or for both signs of sample bias. NDR for positive sample bias has also been observed independently by Bedrosssian *et al.*[21] In Fig. 9 we show how spacially localized NDR is. Using our ARTS setup, I–V curves are obtained 3 Å apart from point A to F. It is clear from Fig. 9 that NDR behavior is localized to a region with a diameter of only $\sim$10 Å.

NDR is the fundamental property of electronic devices such as the Esaki diode,[22] and of quantum wells or dots[19] and can be used to build oscillators, switches, and logical devices. The atomic sites we studied behave like tunnel diodes or atomic size quantum dots whose active region involves just two atomic-size sites: one on the surface and the other the atom on the tip through which the tunneling current flows. In the following we will explore the mechanisms by which NDR may develop on the atomic scale.

On the basis of measurements on partially oxidized Si, it

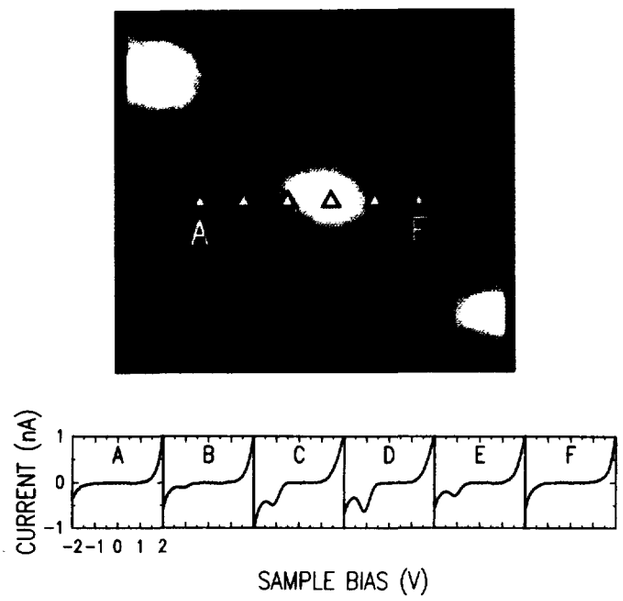

FIG. 9. Top: STM topograph showing a defect site whose I–V curve shows negative differential resistance. Bottom: I–V curves obtained at different points A to F across the above defect site. The points are spaced 3 Å apart.

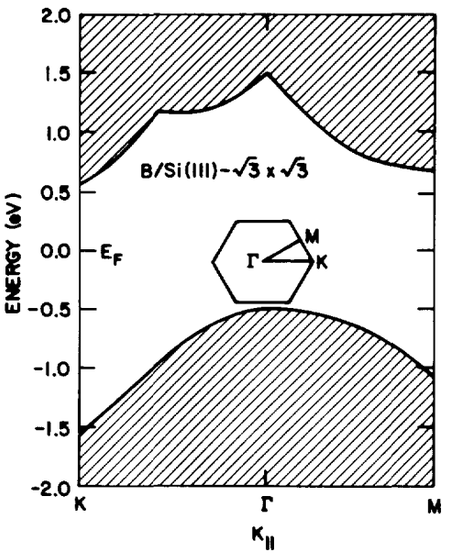

FIG. 10. Projected bulk states of B/Si(111)-$\sqrt{3}\times\sqrt{3}$. The surface Brillouin zone is shown as inset.

has been proposed that NDR can develop by a "Coulomb-blockade" (CB) mechanism.[23] A CB develops when, e.g., an electron emitted by the tip becomes trapped on a surface site for a sufficiently long time so that it Coulombically repels another tunneling electron. If the Coulomb repulsion between the two electrons is U, then the energy gained by a tunneling electron upon reaching this charged site is not eV_{EXT}, where V_{EXT} is the externally applied bias, but $eV_{\mathrm{EXT}} - U$. If $eV_{\mathrm{EXT}} < U$, then the tunneling electron will arrive at a level below the Fermi energy of the sample and tunneling thus will be suppressed. A typical value of U for Si db-type of states is ~ 0.5 eV.[24] In the CB mechanism[23] the energies of the peaks in the I–V curves (b) and (c) of Fig. 8 are interpreted as the energies of electron trap states at $+1.5$ and -1.5 eV relative to E_F, respectively. However, according to band-structure calculations[25] (see Fig. 10), the energies $eV_{\mathrm{EXF}} - U$ for both the $+1.5$ and -1.5 eV states are within the bulk conduction and valence bands of the crystal so that no CB should develop. The trapping times required for CB to develop are determined by the maximum tunneling rate which is about $5\times 10^{9}\ \mathrm{s}^{-1}$ in our experiments. Thus, extremely small widths of $\sim 10^{-6}$ eV are required. It is difficult to see why the states at $+$ or -1.5 eV, well within the bulk bands, will not be broadened by hybridization with bulk states. More detailed studies of NDR as a function of set-current and set-voltage to be published elsewhere[26] provide further evidence against the CB mechanism in this case. It is also important to note that high binding energy states within the valence band such as the -1.5 eV state are in general not good candidates for observing CB effects. The tunneling current is dominated by contributions from states near E_F because, in this case, the tunneling barriers are the lowest. Finally, it is hard to see how a CB mechanism can account for the I–V behavior seen in Fig. 8(d). From the above discussion it is clear that CB is not a likely mechanism for the development of NDR in the B/Si(111) system.

We propose that a general mechanism by which NDR can develop on the atomic scale involves the characteristics of the energy level spectra of the sample and the STM tip. The tunneling current in the STM depends on both the convolution of sample and tip density of states (DOS) and the transmission probability (T) as indicated by

$$I \propto \int_{E_F}^{E_F+eV} \mathrm{DOS}_S(\mathbf{r},E)\,\mathrm{DOS}_T(\mathbf{r},E-eV)\,T(\mathbf{r},E,eV)\,dE. \tag{1}$$

We have observed NDR only over isolated, minority sites of the B/Si(111) surface. Such sites have relatively narrow DOS spectra. The tip DOS is a function of the tip structure and composition. Under the conditions where NDR was observed, atomic resolution was maintained. This suggests that tunneling involves a single atom on the STM tip. It is obvious then that the DOS of the bulk metal from which the tip is made should not provide a good representation of the DOS of the active area of the tip. One would expect[27] a peaked distribution, most probably a Lorentzian with a width that depends on the coupling of the "active area" to the rest of the tip. This coupling can be quite weak, and the corresponding DOS spectrum quite narrow if the active area of the tip is composed of an adatom or small cluster of atoms of different chemical nature than that of the bulk of the tip. Foreign atoms on the tip may be present from the tip preparation process (e.g., metal oxides or carbides), from exposure of the sample to reactants, or through unintentional contact of the tip with the sample surface. Evidence for the importance of the tip in the development of NDR is provided by two types of observations: (a) NDR is not always observable over a particular type of site, but depends on the tip whose structure varies even within a single experiment as atoms

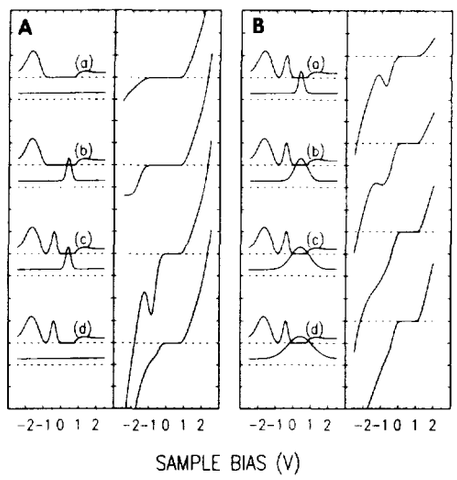

FIG. 11. Computer simulations of I–V characteristics. The barrier height and the tip-to-surface distance are 4eV and 8Å, respectively. (A) Left: DOS of sample (top) and tip (bottom). Right: Resulting I–V curves. (B) The role of the width of the tip DOS in the development of negative differential resistance.

move on its surface; (b) NDR can be observed even over sites of a clean surface such as the restatom sites of Si(111)-7×7 if, e.g., the tip is driven into the surface and is presumably coated by Si atoms. We propose that whenever both the sample and the tip have relatively narrow DOS features of the appropriate energy, tunneling between them may lead to NDR. We illustrate this by the computer simulations shown in Fig. 11. In Fig. 11(A) (left) the DOS of the sample (top) and tip (bottom) are shown and in Fig. 11(A) (right) the resulting I–V curves. It is clear that NDR at negative bias develops only when tunneling involves relatively narrow peaks in the DOS of both sample and tip. In this picture the peaks in the I–V curves showing NDR do not correspond to the energies of trap states as in the CB model, but instead appear when the bias is such that the DOS peaks of the sample and tip have the same energy [curves (b) and (c) in Fig. 8], or when the Fermi level crosses a peak in the DOS spectrum [curve (d) in Fig. 8]. In Fig. 11(B) we illustrate how the NDR behavior depends on the width of the tip DOS spectrum.

The above discussion has important implications on the interpretation of ARTS spectra in general. Clearly, it is not safe to assume that the structure observed in ARTS spectra is simply due to the DOS of the sample; any structure in the tip DOS will also be reflected in the spectra. This is particularly true in the high binding energy region of the occupied states spectrum. The transmission coefficient T [see Eq. (1)] for tunneling out of such sample states is very low and structure in the tip DOS can dominate the spectrum. Thus, it is important that the origin of structure in ARTS spectra be carefully established in repeated experiments and by studying surface structures whose spectral characteristics have already been established.

V. SUMMARY AND CONCLUSIONS

In conclusion, we have determined the details of the interaction of B with Si(111) surfaces and its effects on surface electronic structure, reconstruction, and chemistry. Specifically, we have been able to image the B-containing molecules on the surface and follow the structural and electronic changes that occur upon thermal annealing. We found that the equilibrium adsorption configuration of B is different from that of other group III atoms and involves a novel structure where B occupies a substitutional site in the third atomic layer directly below a Si adatom. The stability of this configuration is due to minimization of subsurface strain and the depopulation of the Si adatom dangling bond by charge transfer to the subsurface B atom. The resulting B/Si(111)-$\sqrt{3}\times\sqrt{3}$ surface is insulating and has no occupied dangling-bond states. This electronic structure is reflected in a unique way in the chemical properties of the Si adatoms comprising the top layer. We illustrated this using the reaction with NH_3 as an example. We found that not only is the reaction rate affected by B-doping but the nature of the reaction itself is different. While NH_3 dissociates at adatom sites of the 7×7 surface, it chemisorbs molecularly and reversibly at adatom sites of the $\sqrt{3}\times\sqrt{3}$ surface. This is a novel short-range doping effect on chemical reactivity which involves direct charge-transfer interaction between the dopant atom and the surface active (i.e., dangling-bond) site.

Finally, we have investigated the electrical characteristics of localized minority sites on the $\sqrt{3}\times\sqrt{3}$ surface. We have found that I–V curves over such sites may show regions of negative differential resistance and that this behavior is localized in areas of atomic dimensions (~ 1 nm). We have examined the possible mechanisms by which negative resistance may develop at the atomic scale and have provided evidence for the operation of a general mechanism which involves tunneling between localized states on surface and tip. The essential requirement for negative resistance to develop is the existance of narrow peaks at appropriate energies in the DOS spectra of the sample and tip. The above observations have important implications on discussions regarding the utimate size-limit of electronic devices. The structures we have investigated behave as tunnel diodes whose active regions involve just two atomic sites—one on the surface and one on the tip.

[1] G. Binnig, H. Rohrer, Ch. Gerber, and E. Weibel, Phys. Rev. Lett. **49**, 57 (1982).
[2] For reviews see G. Binnig and H. Rohrer, Rev. Mod. Phys. **57**, 615 (1987); P. K. Hansma and J. Tersoff, J. Appl. Phys. **61**, R1 (1987); G. P. Kochanski, Annu. Rev. Mater. Sci. (to be published).
[3] For a review see: R. J. Hamers, Annu. Rev. Phys. Chem. **40**, 531 (1989).
[4] R. J. Hamers and J. E. Demuth, Phys. Rev. Lett. **35**, 2527 (1988).
[5] J. M. Nicholls, B. Reihl, and J. E. Northrup, Phys. Rev. B **35**, 4137 (1987).
[6] J. Nogami, S. Park, and C. F. Quate, Phys. Rev. B **36**, 6221 (1987).
[7] In-Whan Lyo, E. Kaxiras, and Ph. Avouris, Phys. Rev. Lett. **63**, 1261 (1989).
[8] Ph. Avouris and R. Wolkow, Phys. Rev. B **39**, 5091 (1989); R. Wolkow and Ph. Avouris, Phys. Rev. Lett. **60**, 1049 (1988).
[9] R. K. Headrick, I. K. Robinson, E. Vlieg, and L. C. Feldman, Phys. Rev. Lett. **63**, 1253 (1989).
[10] P. Bedrossian, R. D. Meade, K. Mortensen, D. M. Chen, and J. A. Golovchenko, Phys. Rev. Lett. **63**, 1257 (1989).
[11] Ph. Avouris, J. Phys. Chem. **94**, 2246 (1990).
[12] K. Takayanagi, Y. Nanishiro, M. Takahashi, H. Motoyoshi, and K. Yagi, J. Vac. Sci. Technol. A **3**, 1502 (1985).

[13] S. Tanaka, M. Onchi, and M. Nishijima, Surf. Sci. **191**, L756 (1987).
[14] L. Kubler, E. K. Hill, D. Bolmont, and G. Gewinner, Surf. Sci. **183**, 503 (1987).
[15] F. Bozso and Ph. Avouris, Phys. Rev. B **38**, 3943 (1988).
[16] H. F. Winters and D. Haarer, Phys. Rev. B **36**, 6613 (1987), and references cited therein.
[17] J. A. Yarmoff and F. R. McFeeley, Phys. Rev. B **38**, 2057 (1988).
[18] F. A. Houle, Phys. Rev. B **39**, 10120 (1989).
[19] *Physics and Technology of Submicron Structures*, Springer Series in Solid State Sciences, edited by H. Henrich, G. Bauer, and F. Kucher (Springer, Berlin, 1988), Vol. 83.
[20] In-Whan Lyo and Ph. Avouris, Science **245**, 1369 (1989).
[21] P. Bedrossian, D. M. Chen, K. Mortensen, and J. A. Golovchenko, Nature **432**, 258 (1989)
[22] L. Esaki, Phys. Rev. B **109**, 603 (1958).
[23] R. J. Hamers and R. Koch, *The Physics and Chemistry of SiO_2 and Si-SiO_2 Interface*, edited by C. R. Helms and B. E. Deal (Plenum, New York, 1988).
[24] W. B. Fowler and R. J. Elliot, Phys. Rev. B **34**, 5525 (1986); J. Stuke, Philos. Mag. B **52**, 225 (1985); J. E. Northrup, Phys. Rev. Lett. **57**, 154 (1986).
[25] E. Kaxiras, K. C. Pandey, F. J. Himpsel, and R. M. Tromp, Phys. Rev. B **41**, 1262 (1990).
[26] In-Whan Lyo and Ph. Avouris (to be published).
[27] N. D. Lang and A. R. Williams, Phys. Rev. B **18**, 616 (1978).